TISSUE ENGINEERING: Part A
Volume 21, Numbers 5 and 6, 2015

DOI: 10.1089/ten.tea.2014.0022

Transplantation of Heterospheroids of Islet Cells and Mesenchymal Stem Cells for Effective Angiogenesis and Antiapoptosis

Jung-Youn Shin, MS,[1,*] Jee-Heon Jeong, PhD,[2,*] Jin Han, MEng,[1] Suk Ho Bhang, PhD,[3] Gun-Jae Jeong, BS,[1] Muhammad R. Haque, MS,[4] Taslim A. Al-Hilal, MS,[5] Myungkyung Noh, BS,[1] Youngro Byun, PhD,[4,5] and Byung-Soo Kim, PhD[1,6]

Although islet transplantation has been suggested as an alternative therapy for type 1 diabetes, there are efficiency concerns that are attributed to poor engraftment of transplanted islets. Hypoxic condition and delayed vasculogenesis induce necrosis and apoptosis of the transplanted islets. To overcome these limitations in islet transplantation, heterospheroids (HSs), which consist of rat islet cells (ICs) and human bone marrow-derived mesenchymal stem cells (hMSCs), were transplanted to the kidney and liver. The HSs cultured under the hypoxic condition system exhibited a significant increase in antiapoptotic gene expression in ICs. hMSCs in the HSs secreted angiogenic and antiapoptotic proteins. With the HS system, ICs and hMSCs were successfully located in the same area of the liver after transplantation of HSs through the portal vein, whereas the transplantation of islets and the dissociated hMSCs did not result in localization of transplanted ICs and hMSCs in the same area. HS transplantation resulted in an increase in angiogenesis at the transplantation area and a decrease in the apoptosis of transplanted ICs after transplantation into the kidney subcapsule compared with transplantation of islet cell clusters (ICCs). Insulin production levels of ICs were higher in the HS transplantation group compared with the ICC transplantation group. The HS system may be a more efficient transplantation method than the conventional methods for the treatment of type 1 diabetes.

Introduction

Islet transplantation is a promising method for the treatment of type 1 diabetes.[1] Although the rate of insulin independence has improved considerably with islet transplantation, the hypoxic condition at the cell transplantation region represents a substantial obstacle to overcome in the early stage of transplantation.[2–6] Capillary density of pancreatic islets is ~10 times higher than that of the exocrine tissue area in the pancreas for an effective insulin secretion response to the glucose level in blood.[7,8] However, this specialized vasculature of islets is disrupted as extracellular matrix and vessels are lost, which inhibits the survival of core cells of islets.[9] As a result, cell viability and function are compromised.[10] The transplanted islets suffer from a hypoxic environment and may lose their viability and function during the early stage of transplantation until vascular network formation occurs ~14 days after the transplantation.[11] Often, more than 50% of the transplanted islets fail in engraftment and undergo programmed cell death and necrosis caused by hypoxia[12]; these factors constitute the major causes of islet cell (IC) death after transplantation.

Mesenchymal stem cells (MSCs) can secrete angiogenic growth factors, thereby contributing to angiogenesis and vasculature stabilization in the cell transplantation region.[13,14] Moreover, MSC cotransplantation can help to prevent graft rejection, since MSCs have immune-modulating properties.[15,16] Thus, researchers have proposed that the islet–MSC composite may have beneficial effects toward improving viability of the grafted islet.[17,18] Johansson *et al.* reported that islet composites with endothelial cells and MSCs have beneficial effects on angiogenesis and immune regulation after

[1]School of Chemical and Biological Engineering, Seoul National University, Seoul, Republic of Korea.
[2]College of Pharmacy, Yeungnam University, Gyeongsan, Gyeongbuk, Republic of Korea.
[3]School of Chemical Engineering, Sungkyunkwan University, Suwon, Republic of Korea.
[4]Department of Molecular Medicine and Biopharmaceutical Sciences, Graduate School of Convergence Science and Technology, Seoul National University, Seoul, Republic of Korea.
[5]Research Institute of Pharmaceutical Sciences, College of Pharmacy, Seoul National University, Seoul, Republic of Korea.
[6]Bio-MAX Institute, Institute for Chemical Processes, Engineering Research Institute, Seoul National University, Seoul, Republic of Korea.
*These authors contributed equally to this work.

transplantation.[19] Sakata *et al.* also reported that the co-transplantation of islets with MSCs has the potential benefit of enhancing angiogenesis and improving islet function.[20] However, transplanted MSCs would be easily washed out into the bloodstream, especially after transplantation through the portal vein of the liver, whereas large-sized islets (diameter = 50–400 μm) would remain. Thus, locating ICs with MSCs at the transplantation site for their effective interaction would be difficult, and transplantation of a mixture of islets and MSCs would not be an ideal method for producing a positive effect of MSCs on islets. This study describes the transplantation of heterospheroids (HSs), which consist of ICs and MSCs, to improve localization of islets with MSCs after transplantation (Fig. 1a), vascularization in the transplantation region, and antiapoptotic activity of the transplanted ICs. To analyze the location of ICs and MSCs, the cells were transplanted through the portal vein of the liver. Additionally, to evaluate the vascularization and cell survival, the cells were transplanted into a subcapsule of the kidney rather than the liver because transplanted cells can be generally localized in the injection area in the kidney and easily retrieved for studying angiogenesis and transplanted cell apoptosis *in vivo*.

Materials and Methods

Isolation of pancreatic islets and dissociation of intact islets

Pancreatic islets were isolated from Sprague-Dawley rats (8 weeks of age, male; Orient Bio, Inc., Seongnam, Republic of Korea) using the collagenase P (Roche Diagnostics, Mannheim, Germany) digestion method [10 mL of solution (0.8 mg/mL) per pancreas]. The islets were cultured in the RPMI-1640 medium (Sigma-Aldrich, St Louis, MO) containing 10% (v/v) fetal bovine serum (FBS; Gibco BRL, Carlsbad, CA), 2 mM sodium bicarbonate, 11 mM glucose (Sigma-Aldrich), 6 mM 4-(2-hydroxyethyl)-1-piperazineethanesulfonic acid (HEPES; Sigma-Aldrich), and 1% (v/v) penicillin/streptomycin (Invitrogen, Carlsbad, CA). Two days after culturing islets, the islets were washed with Hanks' balanced salt solution (HBSS, pH 7.4; Sigma-Aldrich) and dissociated into single cells by suspending them in 0.25% (w/v) trypsin-EDTA (Gibco BRL) at 37°C for 10 min. The dissociated ICs were washed at least twice with cold HBSS. All of the animal experiments were performed with the approval of the Institute of Laboratory Animal Resources, Seoul National University (IACUC No. SNU-070822-5).

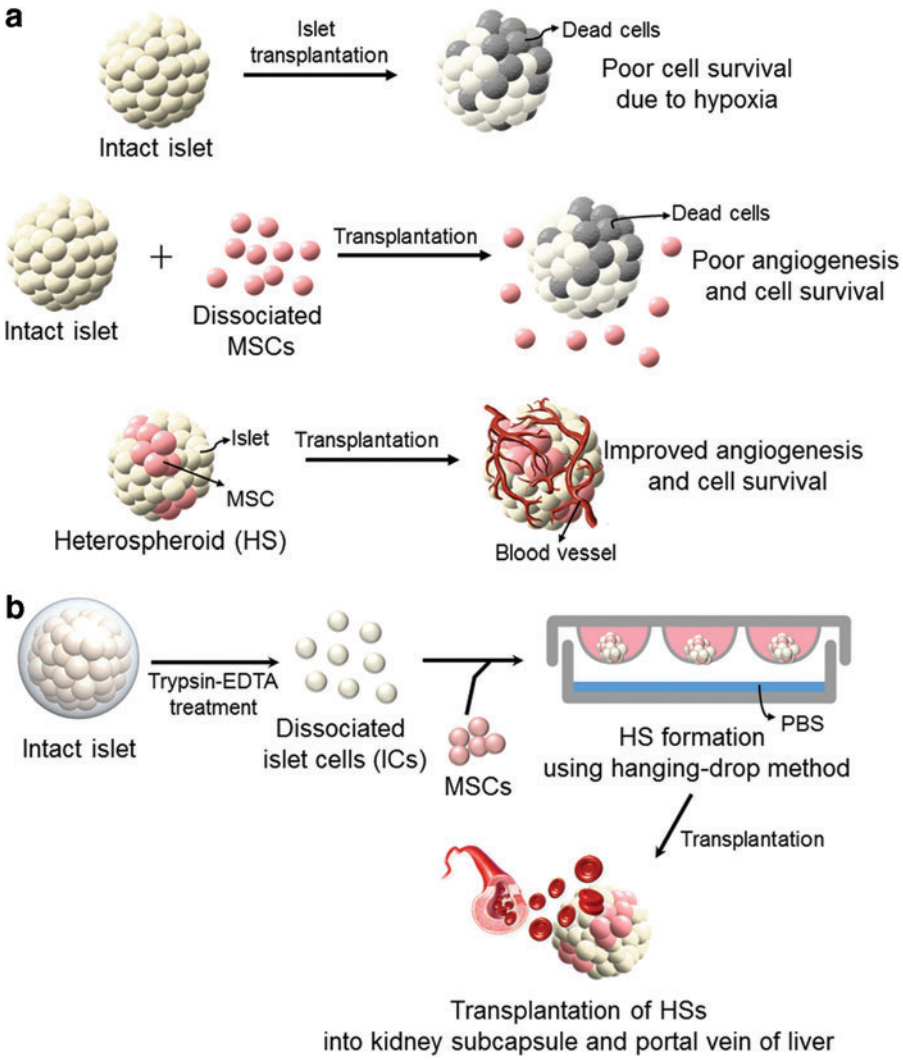

FIG. 1. Schematic illustration showing **(a)** an efficient method of cotransplantation of islets and MSCs for improved angiogenesis and IC survival and **(b)** a protocol for the formation of HSs of ICs and MSCs. **(a)** Islet transplantation often results in poor islet survival due to hypoxia in the transplantation region. Cotransplantation with MSCs can induce angiogenesis and improve IC survival. Importantly, transplantation of HSs of ICs and MSCs would be more effective for locating ICs with MSCs, angiogenesis, and IC survival than in the transplantation of islets and dissociated MSCs. **(b)** HS consisting of rat ICs and hMSCs can be prepared using the hanging-drop method. hMSCs, human bone marrow-derived mesenchymal stem cells; HSs, heterospheroids; IC, islet cell; MSCs, mesenchymal stem cells. Color images available online at www.liebertpub.com/tea

MSC culture

Human bone marrow-derived mesenchymal stem cells (hMSCs; Lonza, Walkersville, MD) were cultured in a 150-mm culture dish with Dulbecco's modified Eagle's medium (DMEM; Gibco BRL) supplemented with 10% (v/v) FBS (Gibco BRL) and 1% (v/v) penicillin/streptomycin (Gibco BRL). The culture medium was changed every other day.

HS and islet cell cluster formation using ICs and hMSCs

To generate HSs and islet cell clusters (ICCs), we used the hanging-drop method with modifications (Fig. 1b).[21] HSs were formed at various cell number ratios of ICs to hMSCs; 10:1, 2:1, and 1:1. Cell suspension solutions were prepared according to the ratio of the different cells (ICs to hMSCs = 10:1, 2:1, and 1:1), but the total cell number concentration was fixed at 2.7×10^4 cells per mL for each group. ICCs and hMSC spheroids were prepared with 2.7×10^4 ICs per mL and 2.7×10^4 hMSCs per mL, respectively. ICs and hMSCs were suspended in DMEM supplemented with 20% (v/v) FBS and 1% (v/v) penicillin/streptomycin (Gibco BRL). Briefly, 30 μL drops of cell suspension were applied to the inside of the lid of a Petri dish containing phosphate-buffered saline (PBS; Sigma-Aldrich) to prevent the cells from drying out. After 72 h of incubation in a 37°C incubator, HSs and ICCs were retrieved using a Pasteur pipette and used for the experiment. The size distributions of HSs and ICCs were determined using Multisizer 3 (Beckman Coulter, Inc., Brea, CA) equipped with a 400 μm aperture.

Viability test of HSs and ICCs

Live/Dead assay (Viability/Cytotoxicity Kit; Molecular Probes, Eugene, OR) was performed for visualizing the viability of HSs and ICCs. HSs and ICCs were stained with calcein AM and ethidium homodimer-1 (EthD-1) dye for 15 min in the dark. Calcein AM stains viable cells, which emit strong green fluorescence, and EthD-1 produces red fluorescence when it encounters dead cells. After washes with HBSS, the fluorescence intensity of islets was detected using a fluorescence microscope (Eclipse TE2000-S; Nikon, Tokyo, Japan). Quantification of live/dead assays was performed with densitometry using Image J software from National Institutes of Health.

Cell composition analysis of HSs

hMSCs were stained with PKH26 (Sigma-Aldrich) before the spheroid formation. When the HS formation was completed, HSs were trypsinized and dissociated single cells were directly counted to determine the cell ratio. Then, the nuclei were counterstained with 4′,6-diamidino-2-phenylindole (DAPI). The cell ratio was determined by the quantification of cell numbers from a minimum of 15 individual images using a fluorescence microscope (IX71 inverted microscope; Olympus, Tokyo, Japan). It is well known that ICs do not proliferate *in vitro*[22–24] and MSCs rarely proliferate in spheroids due to the contact inhibition,[25,26] therefore, the cell ratios of HSs were considered to be constant.

To visually analyze the cell distribution in HSs, hMSCs were labeled with PKH26 and ICs were stained with PKH67 (Sigma-Aldrich) before HS formation. After the HS formation was completed, HSs were collected and fixed with 4% (w/v) paraformaldehyde (PFA; Sigma-Aldrich) for 30 min. PKH26 and PKH67-labeled cells were visualized using a confocal scanning laser microscope (Carl Zeiss-lSM510; Carl Zeiss International, Oberkochen, Germany). Confocal z-stack images, which comprised 10 pictures, were merged to produce a picture for the analysis.

Angiogenic factor secretion analysis

For plating the equal number of ICs, 55 clusters of HSs (10:1) per well and 50 clusters of ICCs per well were plated into a 24-well culture plate containing Millicell culture inserts (Millipore, Billerica, MA). The cells were cultured for 7 days and the cell culture supernate was collected every other day. Angiogenic factors in the supernate were analyzed using the Proteome Profiler™ Human Angiogenesis Antibody Array (R&D Systems, Minneapolis, MN) according to the manufacturer's instructions. Cell culture supernate was diluted and mixed with a detection antibody cocktail and incubated with a capture antibody-arrayed membrane overnight at 4°C. After washing, the membrane was incubated with HRP-conjugated streptavidin and visualized with chemiluminescence (Kodak, Rochester, NY). The level of human vascular endothelial growth factor (VEGF) in the collected cell culture supernate was also determined using an enzyme-linked immunosorbent assay kit (ELISA; R&D Systems) according to the manufacturer's instructions. To ensure that there is no cross-reactivity of the kit to rat VEGF, the VEGF release profile of ICCs was analyzed as a control.

Transplantation of HSs and ICCs

BALB/C nude mice (Orient Bio, Inc.) were anesthetized with an intraperitoneal injection of ketamine (80 mg/kg) and xylazine (16 mg/kg). HSs (10:1, 2200 clusters) and ICCs (2000 clusters) were transplanted in the subrenal capsule space ($n = 6$). To investigate localization of ICs and hMSCs in the liver, 600 clusters of HSs (ICs:hMSCs = 10:1, hMSCs = 4.0×10^4 cells) or 400 clusters of ICCs with hMSCs (4.0×10^4 cells) were injected into the portal vein ($n = 5$). ICs and hMSCs were labeled with PKH26 and PKH67, respectively, before transplantation. The surgical procedure was considered successful if no bleeding occurred during the surgical procedure.

Immunohistochemistry

The organs with cell transplantation were retrieved 14 and 28 days after the treatment. Samples were dehydrated with a graded ethanol series and embedded in paraffin. The specimens were sliced into 4-μm-thick sections for histological analysis. For the quantification of microvessel density in the transplantation region, the sections were subjected to immunofluorescent staining with anti-CD31 (Abcam, Cambridge, United Kingdom) and anti-insulin (Abcam). After washing with PBS, the slides were incubated with FITC-conjugated (Jackson Immuno Research Laboratories, West Grove, PA) and rhodamine-conjugated secondary antibodies (Jackson Immuno Research Laboratories) to visualize anti-CD31 and anti-insulin signals, respectively. The sections were mounted using mounting solution containing

DAPI (Vecta Laboratories, Burlingame, CA). Images were taken with a fluorescence microscope (IX71 inverted microscope). Whole-mount staining of transplanted islets using anti-CD31 (Abcam) and anti-insulin (Abcam) was performed as described in a previous study.[27] The images were taken with a confocal scanning laser microscope (Carl Zeiss-lSM510; Carl Zeiss International).

Histological examination for hMSC localization in the liver

To examine localization of ICs and hMSCs in the liver, the livers were retrieved 7 days after transplantation. Samples were dehydrated with a graded ethanol series and embedded in paraffin. The specimens were sliced into 4-μm-thick sections. The sections were mounted using mounting solution containing DAPI (Vecta Laboratories) to detect fluorescently labeled hMSCs and ICs. For quantification of hMSC localization with ICs, 200 sections were obtained per liver sample ($n = 5$ livers/group) and 50 sections were randomly picked and analyzed with a fluorescence microscope (IX71 inverted microscope).

Reverse transcriptase–polymerase chain reaction

Cells or tissue samples were homogenized and lysed in TRIzol reagent (Invitrogen). Total RNA was extracted with chloroform (Sigma-Aldrich) and precipitated with 80% (v/v) isopropanol (Sigma-Aldrich). After the supernatant was removed, the RNA pellet was washed with 75% (v/v) ethanol, air-dried, and dissolved in 0.1% (v/v) diethyl pyrocarbonate-treated water (Sigma-Aldrich). The total RNA concentration was determined using a NanoDrop spectrometer (ND-2000; NanoDrop Technologies, Wilmington, DE). Reverse transcription was performed using 1 μg of pure total RNA and Superscript II reverse transcriptase (Invitrogen), and the synthesized cDNA was amplified by reverse transcriptase–polymerase chain reaction (RT-PCR). Quantitative RT-PCR (qRT-PCR) was performed using the StepOnePlus real-time PCR system (Applied Biosystems, Foster City, CA). TaqMan® Master Mix (Applied Biosystems) was used for the reaction. The profiles of gene expression in ICs of spheroids or transplantation area were quantified with TaqMan Gene Expression Assays (Applied Biosystems). For each target, we used rat glyceraldehyde 3-phosphate dehydrogenase (*GAPDH*): Rn01775763_g1 (Reference sequence: NM_017008.3), *Bax*: Rn02532082_g1 (Reference sequence: NM_017059.1), and *Bcl-2*: Rn99999125_m1 (Reference sequence: NM_016993.1). Rat-specific primers were used to investigate the ICs only. The expression level of the target genes was determined using the comparative Ct method, whereby the target was normalized to the endogenous reference (*GAPDH*).[28] Relative gene expressions of ICs in spheroids cultured under normoxic and hypoxic conditions were evaluated. All of the data were analyzed using the $2^{-\Delta\Delta Ct}$ method. RT-PCR was conducted for 35 cycles of denaturing (94°C, 30 s), annealing (60°C, 45 s), and extension (72°C, 45 s) with a final extension at 72°C for 10 min. PCR products were visualized by electrophoresis on a 1% (w/v) agarose gel using RedSafe™ (iNtRON Biotechnology, Kyungki-Do, Korea) staining. The products were analyzed with a gel documentation system (Gel Logic 2200 Pro; Carestream Health, Rochester, NY), and *β-actin* served as an internal control. The sequences of the primers were as follows: human-specific *β-actin*, forward primer 5′-GCA TCT TTC CAG CCT TCC TTC C-3′ and reverse primer 5′-TCA CCT TCA CCG TTC CAG TTT TT-3′; human-specific hypoxia inducible factor-1α (*HIF-1α*), forward primer 5′-ACT TCT GGA TGC TGG TGA TT-3′ and reverse primer 5′-TCC TCG GCT AGT TAG GGT AC-3′. Human-specific primers were used to investigate hMSCs only.

Western blot analysis

The samples were lysed using a Dounce homogenizer (50 strokes, 4°C; Kontes, Vineland, NJ) in an ice-cold lysis buffer [15 mM Tris HCl (pH 8.0), 0.25 M sucrose, 15 mM NaCl, 1.5 mM $MgCl_2$, 2.5 mM EDTA, 1 mM EGTA, 1 mM dithiothreitol, 2 mM NaPPi, 1 μg/mL pepstatin A, 2.5 μg/mL aprotinin, 5 μg/mL leupeptin, 0.5 mM phenylmethylsulfonyl fluoride, 0.125 mM Na_3VO_4, 25 mM NaF, and 10 μM lactacystin]. Protein concentration was determined using a bicinchoninic acid (BCA) protein assay (Pierce Biotechnology, Rockford, IL). Equal protein concentrations from each sample were mixed with a sample buffer, loaded, and separated by sodium dodecyl sulfate–polyacrylamide gel electrophoresis (SDS-PAGE) on a 10% (v/v) resolving gel. The proteins separated by SDS-PAGE were transferred to an Immobilon-P membrane (Millipore) and subsequently probed with antibody against caspase-7 (Santa Cruz Biotechnology, Santa Cruz, CA), caspase-3 (LifeSpan Biosciences, Seattle, WA), insulin (Abcam), and β-actin (Abcam) for 1 h at room temperature. Then, the membranes were incubated with horseradish peroxidase-conjugated secondary antibody (Santa Cruz) for 1 h at room temperature. The blots were developed using an enhanced chemiluminescence detection system (Amersham Bioscience, Piscataway, NJ). Luminescence was recorded on X-ray film (Fuji super RX; Fujifilm Medical Systems, Tokyo, Japan), and bands were imaged and quantified with an Imaging Densitometer (Bio-Rad, Hercules, CA).

Statistical analysis

Quantitative data are expressed as mean ± standard deviation. Statistical analysis comparisons were conducted using the Bonferroni test. A value of $p < 0.05$ was considered to be statistically significant.

Results

Formation of ICCs and HSs

ICs and hMSCs were aggregated using the hanging-drop method within 3 days. ICCs and HSs showed round-shaped spheroids, and the live/dead assay demonstrated that most of the cells of ICCs and HSs were viable (Fig. 2a). Although a few dead cells were detected in ICCs, almost all of the aggregates emitted strong green fluorescence as an indicator of good viability. The diameters of ICCs, HSs, (ICs:hMSCs = 10:1), HSs (2:1), and HSs (1:1) were 81.4 ± 64.3, 78.7 ± 49.7, 100.4 ± 55.7, and 80.6 ± 48.3 μm, respectively (Fig. 2b). No significant difference among the groups was found.

Confocal laser scanning microscopy images showed that HSs comprised ICs and hMSCs (Fig. 2c). Among the mixture of ICs and hMSCs, the cells with the same characteristics preferentially aggregated first, and subsequently, the cell aggregates heterogeneously adhered to each other, forming HSs. A quantitative analysis on the cell composition ratio of ICs to

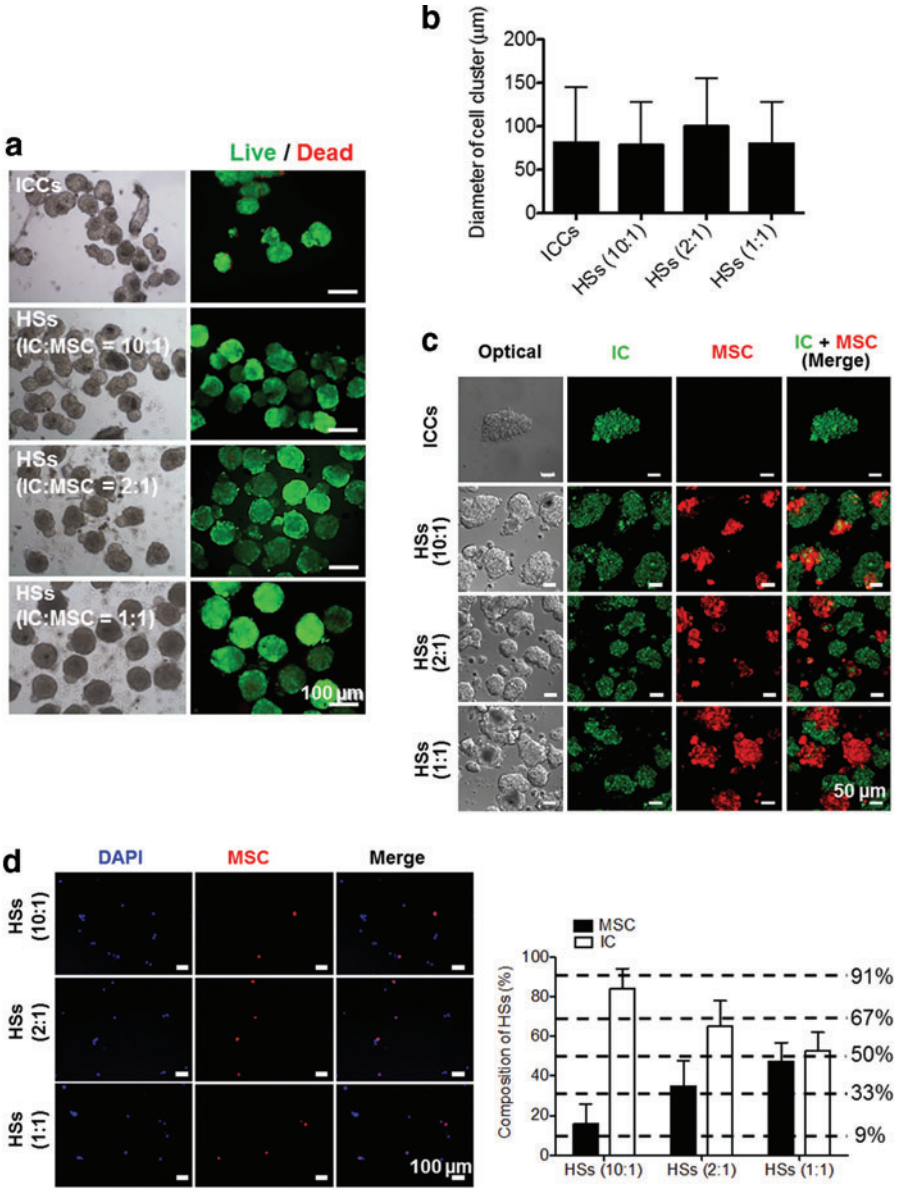

FIG. 2. Characteristic analysis of ICCs and HSs after complete aggregation. **(a)** Light microscopic (*left*) and live/dead cell (*right*) images of ICCs and HSs. *Green* and *red* signals indicate live and dead cells, respectively. Scale bars = 100 μm. **(b)** The diameters of ICCs and HSs with various ICs/hMSCs ratios of 10:1, 2:1, and 1:1. There was no statistical significance between any two groups. **(c)** Confocal laser scanning microscopic images of cell clusters (*green*: ICs; *red*: hMSCs). Scale bars = 50 μm. **(d)** Cell images after dissociation of HSs into ICs and hMSCs (*left panel*, *blue*: DAPI, *red*: hMSCs) and cell composition (*right panel*). Scale bars = 100 μm. DAPI, 4′,6-diamidino-2-phenylindole; ICCs, islet cell clusters. Color images available online at www.liebertpub.com/tea

hMSCs showed that HSs preserved the initial ratio of ICs to hMSCs in cell suspension (Fig. 2d). hMSC ratios to the total cells in HSs (10:1), HSs (2:1), and HSs (1:1) were 14.2% ± 9.9%, 33.7% ± 8.6%, and 45.9% ± 9.3%, respectively.

Attenuated apoptosis of ICs in HSs in vitro

To evaluate the comparative long-term viability of HSs and ICCs, live/dead analysis was performed on day 7 (Fig. 3a). Cells in spheroids showed comparatively high viability. Cell aggregation did not show much difference in live/dead images among ICCs and HSs.

The viability of ICCs and HSs cultured for 2 days under normoxic (20% oxygen) and hypoxic (1% oxygen) conditions was compared (Fig. 3b), and their apoptotic and antiapoptotic gene expression levels were analyzed with qRT-PCR (Fig. 3c). Hypoxic condition was set to mimic the *in vivo* hypoxic environment after IC transplantation.[29,30] The live/dead images of ICCs and HSs under normoxic condition did not show much difference between ICCs and HSs (10:1) (Fig. 3a, b). However, in the hypoxic condition, hMSCs in HSs relieved islet apoptosis. The ICC group showed relatively more dead signals compared with the HS group. As shown in Figure 3b, under hypoxic condition, the dead signal area of MSC spheroids was significantly smaller that of ICCs. This result suggests that it is highly possible that ICs, rather than MSCs, in HSs show the dead signals in the hypoxic condition.

The apoptotic and antiapoptotic gene expressions of rat ICs were investigated using rat-specific primers (Fig. 3c). *Bax*, an apoptotic gene, was downregulated in HSs (10:1), HSs (2:1), and HSs (1:1) compared with ICCs (0.6 ± 0.1, 0.4 ± 0.1, and 0.6 ± 0.1, respectively), whereas *Bcl-2*, an antiapoptotic gene, was significantly upregulated in HSs (10:1), HSs (2:1), and HSs (1:1) compared with ICCs (5.3 ± 0.7, 2.0 ± 0.5, and 3.9 ± 0.1, respectively). Spheroids cultured under the hypoxic condition demonstrated that *Bcl-2* expression was upregulated in HSs (10:1) compared with ICCs.

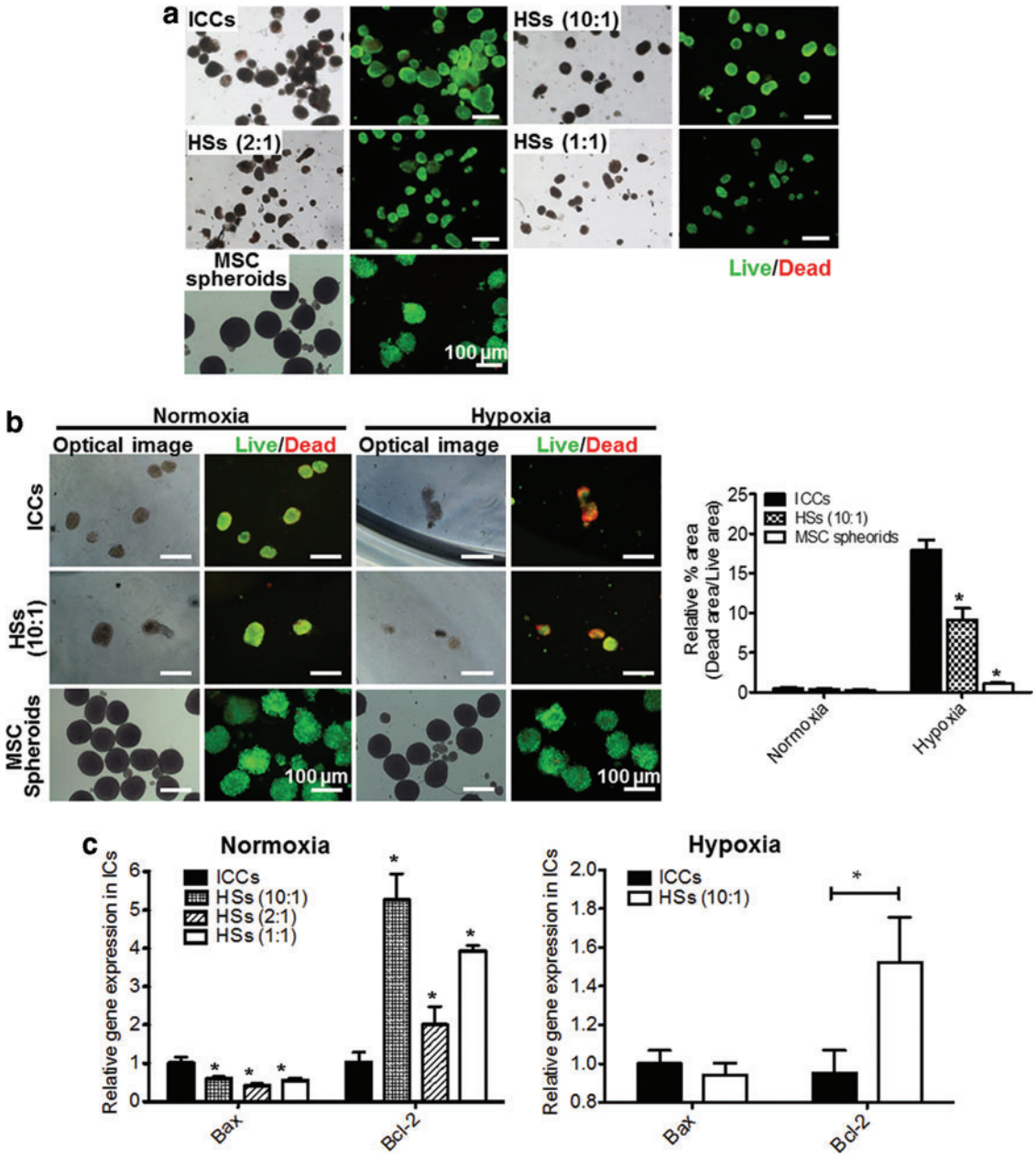

FIG. 3. *In vitro* viability and apoptosis of cultured HSs, ICCs, and hMSC spheroids. **(a)** Long-term *in vitro* viability of ICCs, HSs, and hMSC spheroids on day 7 as evaluated by live/dead assay. Scale bars = 100 μm. **(b)** Live/dead images (*left panel*) and their relative quantification graph (*right panel*) of ICCs, HSs (10:1), and hMSC spheroids cultured under normoxic and hypoxic conditions for 2 days. *Green* and *red signals* indicate live and dead cells, respectively. Scale bars = 100 μm. $*p < 0.05$ compared with ICCs. **(c)** Relative expression of *Bax* and *Bcl-2* of ICs in ICCs or HSs cultured under normoxic or hypoxic condition, as evaluated by qRT-PCR. $*p < 0.05$ compared with ICCs. qRT-PCR, quantitative reverse transcriptase-polymerase chain reaction. Color images available online at www.liebertpub.com/tea

Selection of appropriate ratio of ICs to hMSCs in HSs

It has been known that cell–cell interaction of ICs is indispensable and is essential for insulin secretory response to control glucose concentration in the blood.[31–33] To reinforce the insulin secretion ability of ICs, the HS (10:1) group was selected as the experimental group in the following experiments. HSs (10:1) have the least number of hMSCs, which ensure a high extent of islet cell–cell interaction and the highest antiapoptotic effect on the ICs (Fig. 3).

Angiogenic factor secretion of HSs

Angiogenic factors produced by HSs (10:1) were investigated with a human angiogenesis antibody array (Fig. 4a). The collected cell culture supernate contained numerous angiogenic factors, such as tissue inhibitor of metalloproteinase-1 (TIMP-1), insulin-like growth factor-binding protein-3 (IGFBP-3), interleukin-8 (CXCL8), and VEGF. The VEGF secretion profile was also investigated with the human VEGF ELISA kit (Fig. 4b). The concentration of VEGF in the HS

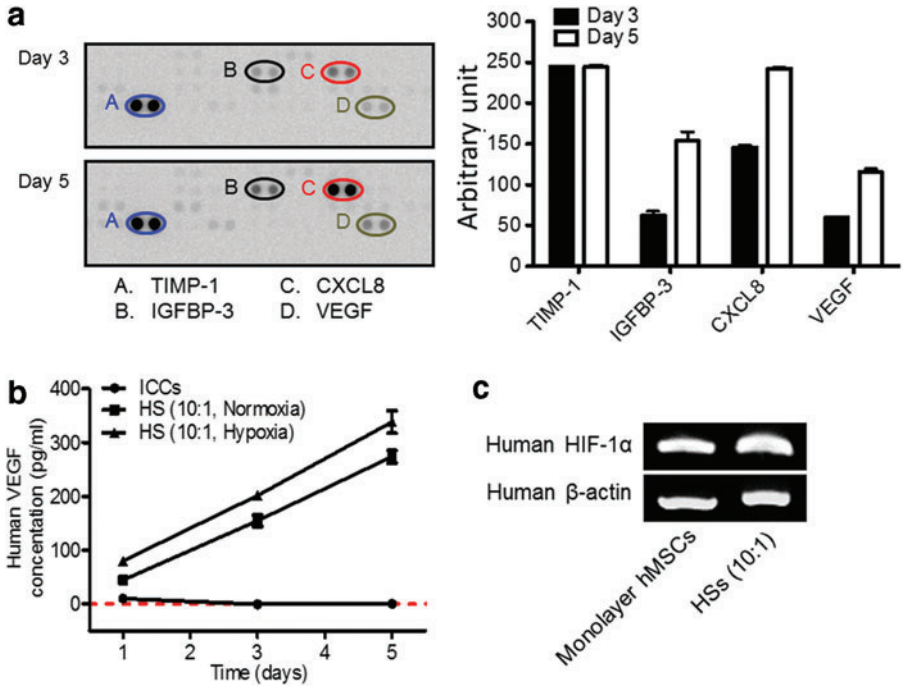

FIG. 4. Analysis of angiogenic factors present in cell culture supernate, and human HIF-1α mRNA expressions in monolayer hMSCs and hMSCs of HSs on day 3. **(a)** The relative amounts of human angiogenic factors (TIMP-1, IGFBP-3, CXCL8, and VEGF) present in cell culture supernate of HSs (10:1). Cell culture supernate was collected on days 3 and 5 and subjected to a human angiogenesis antibody array. Since the data represent the average values from a single test, which yielded two test values for each individual cytokine, statistical significance was not determined. **(b)** The amounts of hVEGF secreted from rat ICCs and HSs (10:1) containing hMSCs and rat ICs cultured in normoxic conditions and HSs (10:1) cultured in hypoxic conditions at various culture time points, as evaluated by ELISA. The *red dashed line* indicates 0 pg/ml of hVEGF. $p < 0.05$ between any two groups at all time points. **(c)** Human HIF-1α mRNA expressions of monolayer hMSCs or HSs on day 3. CXCL8, interleukin-8; ELISA, enzyme-linked immunosorbent assay; HIF-1α, hypoxia inducible factor-1α; hVEGF, human vascular endothelial growth factor; IGFBP-3, insulin-like growth factor-binding protein-3; TIMP-1, tissue inhibitor of metalloproteinase-1; VEGF, vascular endothelial growth factor. Color images available online at www.liebertpub.com/tea

group increased gradually in normoxic and hypoxic conditions. Relatively higher quantity of VEGF was secreted from MSCs under hypoxic culture condition. hMSCs in HSs expressed a higher level of HIF-1α mRNA compared with monolayer MSCs, indicating hypoxic condition in spheroids on day 3 (Fig. 4c).

Localization of ICs and hMSCs in the liver

Either the ICCs with dissociated hMSCs or the HSs (10:1) alone were transplanted through the portal vein of the liver, and the livers were retrieved 7 days after the transplantation. In average, 10–30 clusters were found in each liver section, and the percentage of both PKH67-positive (hMSC) and PKH26-positive (IC) clusters were evaluated from total clusters in each liver. The result indicated that intraportally transplanted HSs showed localization of ICs with hMSCs in the same area of the liver (Fig. 5). However, when ICCs and dissociated hMSCs were transplanted, hMSCs were not observed near the transplanted ICCs. This result indicated that only the HS transplantation can systemically localize the hMSCs around the ICs in the transplantation site and can maximize the hMSC effects on islets post-transplantation.

Enhanced angiogenesis near ICs by transplantation of HSs

The angiogenic ability of transplanted ICCs and HSs (10:1) was evaluated by determining the density of CD31-positive cells in the insulin-positive transplanted islet area on days 14 and 28 of transplantation (Fig. 6a). On day 14, CD31-positive cells were detected in the HS-transplanted kidney group. On day 28, the density of CD31-positive cells was significantly increased in the HS transplantation group compared with the ICC transplantation group (Fig. 6a, b). In the ICC transplantation group, CD31-positive cells were slightly detected in the transplantation area on day 28, but the density of the ICC transplantation group was lower than that of the HS transplantation group. These results demonstrate that localization of ICs with MSCs stimulated the vascularization in the islet transplantation area by the angiogenic growth factors released from hMSCs.

Attenuated apoptosis and higher insulin content of ICs by HS transplantation

The rat-specific gene expression of *Bcl-2* (Fig. 7a) and protein expression of cleaved caspase-3, caspase-3, caspase-7

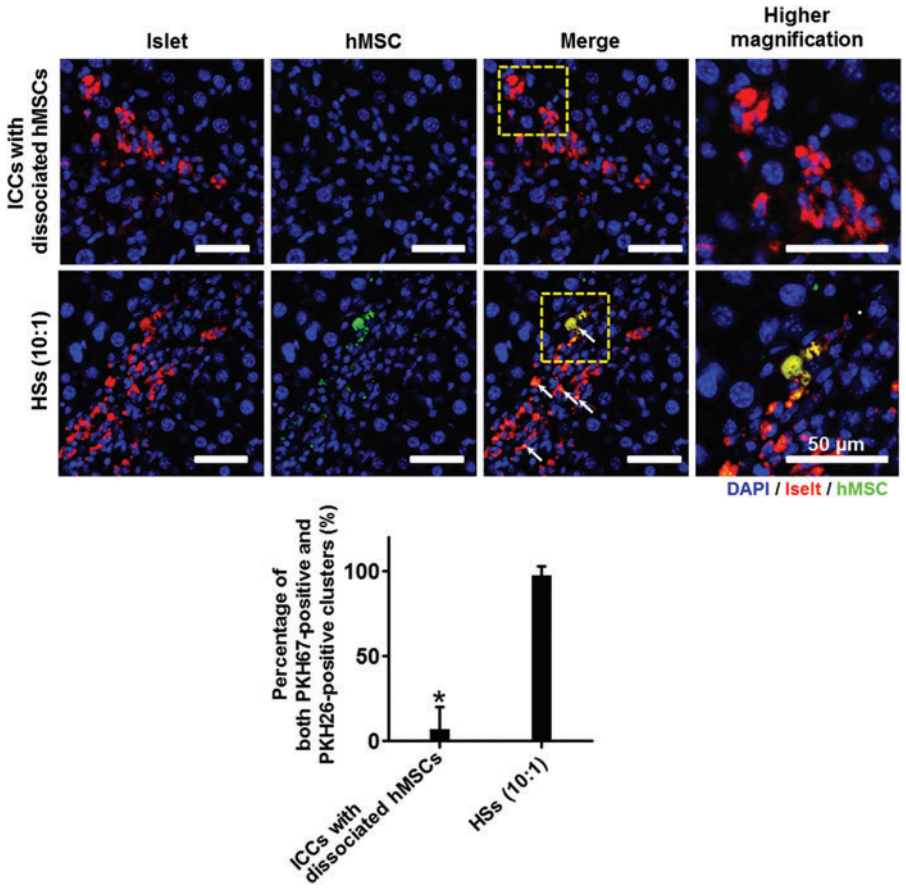

FIG. 5. ICs and hMSC localization in the portal vein of the liver. Before transplantation, ICs and hMSCs were labeled with PKH26 (*red*) and PKH67 (*green*), respectively. The livers were harvested 7 days after transplantation. *Arrows* indicate the ICs localized with hMSCs in the liver. *Blue* indicates nuclei stained with DAPI. Scale bars = 50 μm. The percentages of both PKH67-positive (hMSC) and PKH26-positive (IC) clusters were evaluated from total clusters found in each liver (*lower panel*). *$p <$ 0.05 compared with HSs (10:1) group. Color images available online at www.liebertpub.com/tea

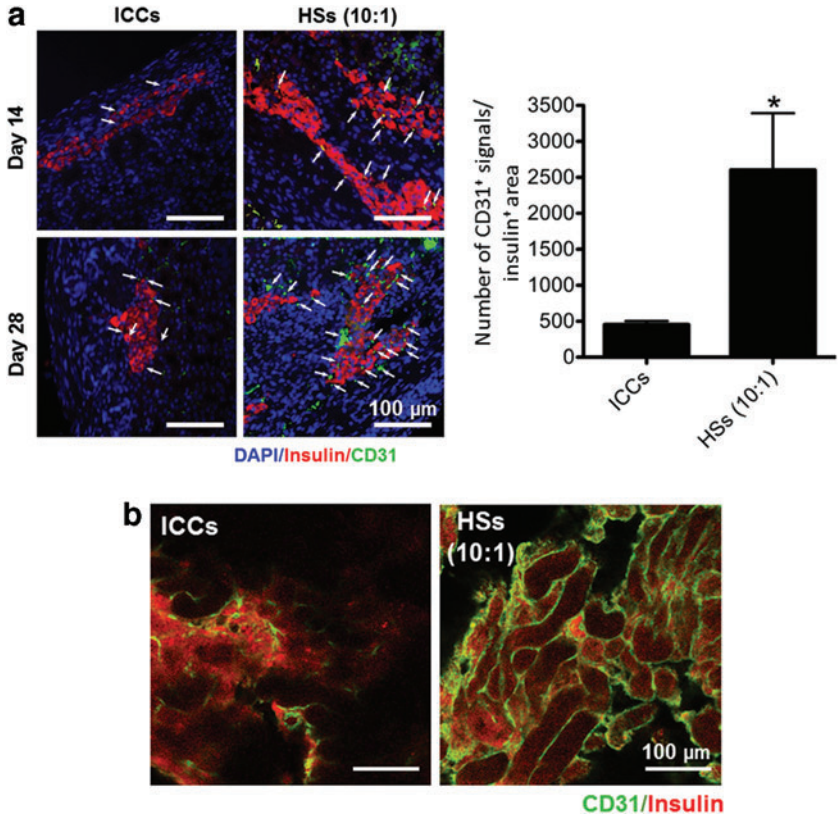

FIG. 6. Angiogenesis at the transplantation area in the kidney subcapsule after transplantation of both ICCs and HSs (IC:hMSC = 10:1). **(a)** CD31-positive (*green*) microvessels with insulin-positive (*red*) transplanted ICs (*left panel*). The kidneys that contained transplanted islets were harvested 14 and 28 days after the transplantation. *Arrows* indicate CD31-positive microvessels in the transplantation region. *Blue* indicates nuclei stained with DAPI. Scale bars = 100 μm. *Right panel*. The density of CD31-positive microvessels in the insulin-positive region. *$p < 0.05$ compared with ICCs. **(b)** Whole-mount immunostaining of CD31 (*green*) and insulin (*red*) in the transplantation area. The kidneys containing transplanted islets were harvested 28 days after the transplantation. Scale bars = 100 μm. Color images available online at www.liebertpub.com/tea

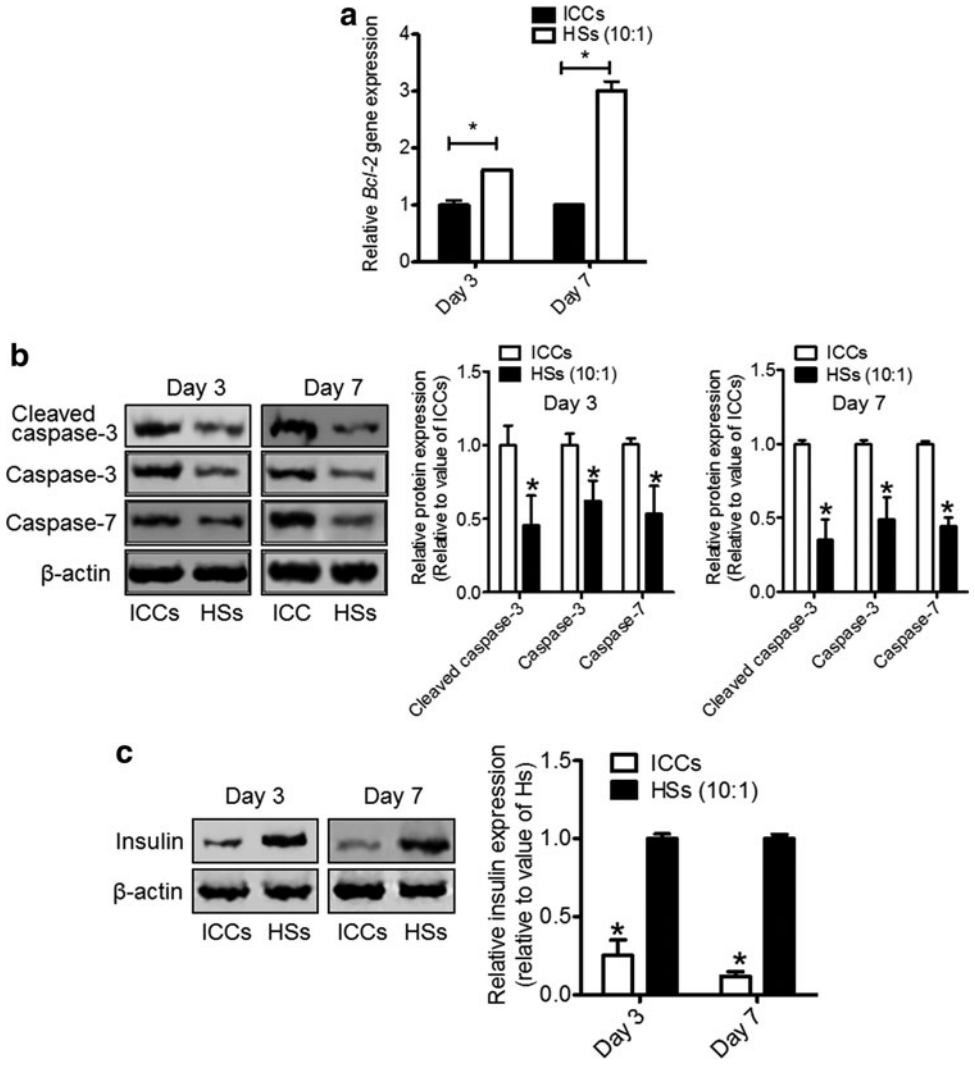

FIG. 7. Evaluation of apoptosis and insulin content of ICCs and ICs in HSs in the transplantation area of the kidneys. **(a)** Relative expression of rat-specific *Bcl-2* of ICCs and ICs in HSs (10:1) as evaluated by qRT-PCR. $*p < 0.05$ compared with ICCs. **(b)** Apoptotic protein expression was evaluated by western blot (*upper panel*) using antibodies against cleaved caspase-3, caspase-3, and caspase-7, and their protein expression levels were evaluated (*lower panel*). $*p < 0.05$ compared with ICCs. **(c)** Insulin content was evaluated by western blot (*left panel*) using antibodies against insulin, and their protein expression levels were evaluated (*right panel*). $*p < 0.05$ compared with HSs.

(Fig. 7b), and insulin (Fig. 7c) of the kidney tissue in the cell transplantation region harvested on days 3 and 7 after the transplantation were analyzed to evaluate the apoptosis and insulin secretion of transplanted rat ICs. In the HS (10:1) transplantation group, rat *Bcl-2* mRNA expression was increased to 1.6 ± 0.8-fold on day 3 and significantly increased to 3.0 ± 0.2-fold on day 7 compared with the ICC transplantation group (Fig. 7a). The protein expression levels of cleaved caspase-3, caspase-3, and caspase-7 were significantly attenuated in the HS (10:1) transplantation group on days 3 and 7 compared with the ICC transplantation group. Moreover, the insulin content of ICs was highly maintained in the HS transplantation group on day 3 and 7 compared with the ICC transplantation group.

Discussion

In the present study, the islet–MSC HS system decreased apoptosis of islets after transplantation (Fig. 7), which could be attributed to factors secreted by MSCs. Previously, Jung *et al.* reported that coculture of islets and MSCs promoted viability and insulin secretory function of islets.[34] Park *et al.* also showed that MSCs secreted various growth factors and increased the viability and the functionality of islets after transplantation.[35] One of the factors secreted by MSCs in HSs, which are responsible for the decreased apoptosis of islets, may be VEGF, a proangiogenic and antiapoptotic factor.[36] VEGF secretion from MSCs in HSs could be stimulated by the mild hypoxic condition in spheroids[37,38] and the insulin secreted by ICs in HSs.[39,40] The upregulation of HIF-1α (Fig. 4c), which can be triggered by the mild hypoxic condition in spheroids, stimulates VEGF expression. Recent studies have shown that HIF-1α can be activated in normoxic conditions in response to various peptide mediators, such as insulin and insulin-like growth factors. Insulin increases the binding affinity of HIF-1α to hypoxia response elements of VEGF and stimulates VEGF secretion.[41]

The transplantation of HSs, which comprised ICs and MSCs, promoted vascularization near the transplanted ICs (Fig. 6), which may improve the viability of the transplanted ICs. The main cause for engraftment failure in islet transplantation is islet damage from the hypoxic condition at the transplantation site. During the islet isolation procedure, islets lose their vasculature of pancreatic islets. Consequently, islets are susceptible to hypoxic injury in the

early periods of transplantation. Generally, blood vessel formation begins 2–4 days after the transplantation and is generally completed after 12–14 days.[39] Delayed and insufficient revascularization would induce necrosis of the transplanted ICs. Preservation of islet viability is the key to prolonging the survival of grafted islets,[19,40] and early islet vasculature formation is crucial for a better transplantation outcome.[42]

The HS system enabled a successful localization of ICs with MSCs after transplantation (Fig. 5), which is responsible for the increased vascularization and decreased apoptosis of ICs. When islets and dissociated MSCs were cotransplanted, we found that MSCs were easily washed away from the transplantation site into the bloodstream (Fig. 5), which would not allow for the angiogenic and antiapoptotic effects of MSCs on the transplanted ICs. In contrast, the HS allowed for the localization of ICs with MSCs after transplantation, and the angiogenic and antiapoptotic factors secreted by the MSCs in HSs would easily affect the adjacent ICs in HSs. Consequently, HS transplantation showed improved blood vessel network formation in the transplantation area and reduced apoptosis of ICs, which may be responsible for the higher insulin expression in the HS transplantation group compared with the ICC transplantation group (Figs. 6 and 7). In this respect, the localization of ICs with MSCs is significant for a successful engraftment and effective insulin secretion outcome of islet transplantation. Therefore, the HS system may be an advantageous delivery method for producing positive effects of MSCs on ICs in contrast to the transplantation of a simple mixture of islets and dissociated MSCs.

Further studies on evaluating the clinical feasibility of this method are necessary. HS formation requires the labor-intensive process of hanging drop, which should be simplified for the clinical application. Recently, several types of devices have been designed and are commercially available alternatives to the hanging-drop method for the convenience of spheroid formation. These devices include AggreWell™ (STEMCELL Technologies, Vancouver, BC, Canada) and Perfecta3D® 384-Well Hanging-Drop Plates (3D Biomatrix, Ann Arbor, MI). Moreover, the long-term survival and functionality of transplanted islets should be examined with glucose-stimulated insulin secretion tests *in vivo* before the clinical application.

The HS formation technology could be expandable to other cell-based therapies. For example, HS of endothelial cells and MSCs could improve angiogenesis compared with single cell type spheroids. Moreover, the HS system can be applied for gene transfection. Transfection of an intact islet is difficult even with viral vector, while dissociated cells are more susceptible for gene transfection. With the HS system, genes can be delivered to nuclei of ICs or MSCs to improve cell functions[43,44] before the spheroid formation, which can make highly functionalized cell clusters for the treatment of type 1 diabetes.

Conclusion

ICs and MSCs localized in the same site after transplantation by transplanting HSs. HSs were formed with the simple hanging-drop method, and the ratio of ICs to MSCs can be easily modified. ICs successfully localized together with MSCs in the liver by HS transplantation. Moreover, HS transplantation resulted in a significantly lower apoptotic activity of ICs and higher angiogenesis near ICs than ICC transplantation. Insulin secretion and deposition were higher in the HS transplantation group compared with the ICC transplantation group. With the HS system, islet transplantation may be more efficient compared with the use of conventional transplantation methods for the treatment of type 1 diabetes.

Acknowledgment

This work was supported by the Seoul National University Brain Fusion Program Research Grant.

Disclosure Statement

No competing financial interests exist.

References

1. Shapiro, A.M., Ricordi, C., Hering, B.J., Auchincloss, H., Lindblad, R., Robertson, R.P., *et al.* International trial of the Edmonton protocol for islet transplantation. N Engl J Med **355,** 1318, 2006.
2. Jeong, J.H., Hong, S.W., Hong, S., Yook, S., Jung, Y., Park, J.B., *et al.* Surface camouflage of pancreatic islets using 6-arm-PEG-catechol in combined therapy with tacrolimus and anti-CD154 monoclonal antibody for xenotransplantation. Biomaterials **32,** 7961, 2011.
3. Gibly, R.F., Graham, J.G., Luo, X., Lowe, W.L., Jr., Hering, B.J., and Shea, L.D. Advancing islet transplantation: from engraftment to the immune response. Diabetologia **54,** 2494, 2011.
4. Goto, M., Tjernberg, J., Dufrane, D., Elgue, G., Brandhorst, D., Ekdahl, K.N., *et al.* Dissecting the instant blood-mediated inflammatory reaction in islet xenotransplantation. Xenotransplantation **15,** 225, 2008.
5. Bennet, W., Groth, C.G., Larsson, R., Nilsson, B., and Korsgren, O. Isolated human islets trigger an instant blood mediated inflammatory reaction: implications for intraportal islet transplantation as a treatment for patients with type 1 diabetes. Ups J Med Sci **105,** 125, 2000.
6. Amiji, M., and Park, K. Surface modification of polymeric biomaterials with poly(ethylene oxide), albumin, and heparin for reduced thrombogenicity. J Biomater Sci Polym Ed **4,** 217, 1993.
7. Henderson, J.R., and Moss, M.C. A morphometric study of the endocrine and exocrine capillaries of the pancreas. Q J Exp Physiol **70,** 347, 1985.
8. Kuroda, M., Oka, T., Oka, Y., Yamochi, T., Ohtsubo, K., Mori, S., *et al.* Colocalization of vascular endothelial growth factor (vascular permeability factor) and insulin in pancreatic islet cells. J Clin Endocrinol Metab **80,** 3196, 1995.
9. Emamaullee, J.A., Rajotte, R.V., Liston, P., Korneluk, R.G., Lakey, J.R., Shapiro, A.M., *et al.* XIAP overexpression in human islets prevents early posttransplant apoptosis and reduces the islet mass needed to treat diabetes. Diabetes **54,** 2541, 2005.
10. Thomas, F.T., Contreras, J.L., Bilbao, G., Ricordi, C., Curiel, D., and Thomas, J.M. Anoikis, extracellular matrix, and apoptosis factors in isolated cell transplantation. Surgery **126,** 299, 1999.

11. Menger, M.D., Yamauchi, J., and Vollmar, B. Revascularization and microcirculation of freely grafted islets of Langerhans. World J Surg **25,** 509, 2001.
12. Biarnes, M., Montolio, M., Nacher, V., Raurell, M., Soler, J., and Montanya, E. Beta-cell death and mass in syngeneically transplanted islets exposed to short- and long-term hyperglycemia. Diabetes **51,** 66, 2002.
13. Jain, R.K. Molecular regulation of vessel maturation. Nat Med **9,** 685, 2003.
14. Yancopoulos, G.D., Davis, S., Gale, N.W., Rudge, J.S., Wiegand, S.J., and Holash, J. Vascular-specific growth factors and blood vessel formation. Nature **407,** 242, 2000.
15. Madec, A.M., Mallone, R., Afonso, G., Abou Mrad, E., Mesnier, A., Eljaafari, A., *et al.* Mesenchymal stem cells protect NOD mice from diabetes by inducing regulatory T cells. Diabetologia **52,** 1391, 2009.
16. Abdi, R., Fiorina, P., Adra, C.N., Atkinson, M., and Sayegh, M.H. Immunomodulation by mesenchymal stem cells: a potential therapeutic strategy for type 1 diabetes. Diabetes **57,** 1759, 2008.
17. Duprez, I.R., Johansson, U., Nilsson, B., Korsgren, O., and Magnusson, P.U. Preparatory studies of composite mesenchymal stem cell islets for application in intraportal islet transplantation. Ups J Med Sci **116,** 8, 2011.
18. Rackham, C.L., Chagastelles, P.C., Nardi, N.B., Hauge-Evans, A.C., Jones, P.M., and King, A.J.F. Co-transplantation of mesenchymal stem cells maintains islet organisation and morphology in mice. Diabetologia **54,** 1127, 2011.
19. Johansson, U., Olsson, A., Gabrielsson, S., Nilsson, B., and Korsgren, O. Inflammatory mediators expressed in human islets of Langerhans: implications for islet transplantation. Biochem Biophys Res Commun **308,** 474, 2003.
20. Sakata, N., Chan, N.K., Chrisler, J., Obenaus, A., and Hathout, E. Bone marrow cell cotransplantation with islets improves their vascularization and function. Transplantation **89,** 686, 2010.
21. Bhang, S.H., Lee, S., Shin, J.Y., Lee, T.J., and Kim, B.S. Transplantation of cord blood mesenchymal stem cells as spheroids enhances vascularization. Tissue Eng Part A **18,** 2138, 2012.
22. Atouf, F., Park, C.H., Pechhold, K., Ta, M., Choi, Y., and Lumelsky, N.L. No evidence for mouse pancreatic beta-cell epithelial-mesenchymal transition *in vitro*. Diabetes **56,** 699, 2007.
23. Chase, L.G., Ulloa-Montoya, F., Kidder, B.L., and Verfaillie, C.M. Islet-derived fibroblast-like cells are not derived via epithelial-mesenchymal transition from Pdx-1 or insulin-positive cells. Diabetes **56,** 3, 2007.
24. Weinberg, N., Ouziel-Yahalom, L., Knoller, S., Efrat, S., and Dor, Y. Lineage tracing evidence for *in vitro* dedifferentiation but rare proliferation of mouse pancreatic beta-cells. Diabetes **56,** 1299, 2007.
25. Abercrombie, M. Contact inhibition and malignancy. Nature **281,** 259, 1979.
26. Pardee, A.B. A restriction point for control of normal animal cell proliferation. Proc Natl Acad Sci U S A **71,** 1286, 1974.
27. Laib, A.M., Bartol, A., Alajati, A., Korff, T., Weber, H., and Augustin, H.G. Spheroid-based human endothelial cell microvessel formation *in vivo*. Nat Protoc **4,** 1202, 2009.
28. La, W.G., Shin, J.Y., Bhang, S.H., Jin, M., Yoon, H.H., Noh, S.S., *et al.* Culture on a 3,4-dihydroxy-l-phenylalanine-coated surface promotes the osteogenic differentiation of human mesenchymal stem cells. Tissue Eng Part A **19,** 1255, 2013.
29. Bhang, S.H., Jung, M.J., Shin, J.Y., La, W.G., Hwang, Y.H., Kim, M.J., *et al.* Mutual effect of subcutaneously transplanted human adipose-derived stem cells and pancreatic islets within fibrin gel. Biomaterials **34,** 7247, 2013.
30. Lehmann, R., Zuellig, R.A., Kugelmeier, P., Baenninger, P.B., Moritz, W., Perren, A., *et al.* Superiority of small islets in human islet transplantation. Diabetes **56,** 594, 2007.
31. Bosco, D., Orci, L., and Meda, P. Homologous but not heterologous contact increases the insulin secretion of individual pancreatic beta cells. Exp Cell Res **184,** 72, 1989.
32. Hauge-Evans, A.C., Squires, P.E., Persaud, S.J., and Jones, P.M. Pancreatic beta-cell-to-beta-cell interactions are required for integrated responses to nutrient stimuli: enhanced Ca2+ and insulin secretory responses of MIN6 pseudoislets. Diabetes **48,** 1402, 1999.
33. Halban, P.A., Powers, S.L., George, K.L., and Bonner-Weir, S. Spontaneous reassociation of dispersed adult rat pancreatic islet cells into aggregates with three-dimensional architecture typical of native islets. Diabetes **36,** 783, 1987.
34. Jung, E.J., Kim, S.C., Wee, Y.M., Kim, Y.H., Choi, M.Y., Jeong, S.H., *et al.* Bone marrow-derived mesenchymal stromal cells support rat pancreatic islet survival and insulin secretory function *in vitro*. Cytotherapy **13,** 19, 2011.
35. Park, K.S., Kim, Y.S., Kim, J.H., Choi, B., Kim, S.H., Tan, A.H., *et al.* Trophic molecules derived from human mesenchymal stem cells enhance survival, function, and angiogenesis of isolated islets after transplantation. Transplantation **89,** 509, 2010.
36. Nör, J.E., Christensen, J., Mooney, D.J., and Polverini, P.J. Vascular endothelial growth factor (VEGF)-mediated angiogenesis is associated with enhanced endothelial cell survival and induction of Bcl-2 expression. Am J Pathol **154,** 375, 1999.
37. Bhang, S.H., Cho, S.W., La, W.G., Lee, T.J., Yang, H.S., Sun, A.Y., *et al.* Angiogenesis in ischemic tissue produced by spheroid grafting of human adipose-derived stromal cells. Biomaterials **32,** 2734, 2011.
38. Dai, Y., Xu, M., Wang, Y., Pasha, Z., Li, T., and Ashraf, M. HIF-1alpha induced-VEGF overexpression in bone marrow stem cells protects cardiomyocytes against ischemia. J Mol Cell Cardiol **42,** 1036, 2007.
39. Griffith, R.C., Scharp, D.W., Hartman, B.K., Ballinger, W.F., and Lacy, P.E. A morphologic study of intrahepatic portal-vein islet isografts. Diabetes **26,** 201, 1977.
40. Davalli, A.M., Ogawa, Y., Ricordi, C., Scharp, D.W., Bonner-Weir, S., and Weir, G.C. A selective decrease in the beta cell mass of human islets transplanted into diabetic nude mice. Transplantation **59,** 817, 1995.
41. Treins, C., Giorgetti-Peraldi, S., Murdaca, J., and Van Obberghen, E. Regulation of vascular endothelial growth factor expression by advanced glycation end products. J Biol Chem **276,** 43836, 2001.
42. Menger, M.D., Jager, S., Walter, P., Hammersen, F., and Messmer, K. A novel technique for studies on the microvasculature of transplanted islets of Langerhans *in vivo*. Int J Microcirc Clin Exp **9,** 103, 1990.

43. Yook, S., Jeong, J.H., Jung, Y.S., Hong, S.W., Im, B.H., Seo, J.W., *et al.* Molecularly engineered islet cell clusters for diabetes mellitus treatment. Cell Transplant **21,** 1775, 2012.
44. Hasegawa, K., Wakino, S., Kimoto, M., Minakuchi, H., Fujimura, K., Hosoya, K., *et al.* The hydrolase DDAH2 enhances pancreatic insulin secretion by transcriptional regulation of secretagogin through a Sirt1-dependent mechanism in mice. FASEB J **27,** 2301, 2013.

Address correspondence to:
Youngro Byun, PhD
Research Institute of Pharmaceutical Sciences
College of Pharmacy
Seoul National University
San 56-1
Sillim 9-Dong
Gwanak-Gu
Seoul 151-742
Republic of Korea

E-mail: yrbyun@snu.ac.kr

Byung-Soo Kim, PhD
School of Chemical and Biological Engineering
Seoul National University
San 56-1
Sillim-Dong
Gwanak-gu
Seoul 151-744
Republic of Korea

E-mail: byungskim@snu.ac.kr

Received: January 9, 2014
Accepted: October 21, 2014
Online Publication Date: January 30, 2015